Dayside Magnetodisk Reconnection in Jovian System: Galileo and Voyager Observation

Jinyan Zhao[1,2] , **Ruilong Guo**[1] , **Quanqi Shi**[1] , **Tao Tang**[1], **Alexander William Degeling**[1] , **Zhonghua Yao**[3,4] , **Denis Grodent**[5] , **Shi-Chen Bai**[1] , **Jong-Sun Park**[1] , **Xiao Ma**[1] , **Junjie Chen**[3] , **Binzheng Zhang**[3] , **Huizi Wang**[1], **Anmin Tian**[1,2] , and **Qiugang Zong**[6]

[1]Shandong Provincial Key Laboratory of Optical Astronomy and Solar-Terrestrial Environment, Institute of Space Sciences, School of Space Science and Physics, Shandong University, Weihai, China, [2]State Key Laboratory of Lunar and Planetary Sciences, Macau University of Science and Technology, Macau, China, [3]Department of Earth Sciences, the University of Hong Kong, Pokfulam, China, [4]Key Laboratory of Earth and Planetary Physics, Institute of Geology and Geophysics, Chinese Academy of Sciences, Beijing, China, [5]Laboratory for Planetary and Atmospheric Physics, STAR Institute, Université de Liège, Liège, Belgium, [6]Institute of Space Physics and Applied Technology, Peking University, Beijing, China

Abstract Magnetic reconnection, an essential mechanism in plasma physics that changes magnetic topology and energizes charged particles, plays a vital role in the dynamic processes of the Jovian magnetosphere. The traditional Vasyliūnas cycle only considers the effect of magnetic reconnection at the nightside magnetodisk. Recently, magnetic reconnection has been identified at the dayside magnetodisk in Saturn's magnetosphere and can impact dayside auroral processes. In this study, we provide the first evidence that the dayside magnetodisk reconnection can also occur at Jupiter. Using data from the Galileo and Voyager 2 spacecraft, we have identified 18 dayside reconnection events with radial distances in the range of 30–60 Jupiter radii (R_J). We analyzed the particle (electron and ion) flux, energy spectra, and characteristic energy of these dayside events and compared them to the nightside events. The statistical results show that the energy spectra and characteristic energy of electrons/ions in dayside and nightside magnetic reconnection events are comparable. On average, the characteristic energy of ions on the dayside is higher than that on the nightside. Based on the limited data set, we speculate that the occurrence rate of dayside magnetodisk reconnection should be significant. The dayside Jovian magnetodisk reconnection seems to have a comparable effect on providing energetic particles as that at nightside and to be one of the key processes driving dynamics within the Jovian magnetosphere.

Plain Language Summary Jupiter has the strongest magnetic field among the planets in our solar system. Particles in the space around Jupiter are affected by its magnetic field. Changes in the strength and structure of the local magnetic field, known as magnetic reconnection, cause those particles to undergo rapid acceleration leading to their energization. In the past, magnetic reconnection was thought to be difficult to occur on Jupiter's dayside magnetodisk. In contrast, the recent observation of reconnection at Saturn's dayside magnetodisk strongly implied the possibility of a similar process at Jupiter. In this paper, taking advantage of the archived data from the Galileo and Voyager 2 spacecraft, we provide the first evidence that the dayside magnetodisk reconnection can occur at Jupiter and have an important effect on the energization of particles.

1. Introduction

At Jupiter, the intense intrinsic magnetic field and rapid rotation (the period is ∼10 hr) impede the access of solar wind particles to the Jovian magnetosphere. Instead, the dominant source of particles is provided by an internal source, the moon Io, which contributes more than ∼1 ton of particles per second to the magnetosphere (e.g., Bagenal, 2007; Delamere et al., 2015; Thomas et al., 2004). This plasma source and the magnetic drag effect produced by Jupiter's fast rotation play pivotal roles in the dynamic processes of Jupiter's magnetosphere. A disc-like ring current takes shape during the outward transport of the Iogenic ions (mainly sulfur and oxygen) (Khurana et al., 2004). The plasma contributed by Io is eventually released from the magnetodisk through magnetic reconnection processes in the magnetotail, as described by the Vasyliūnas cycle (Khurana et al., 2004; Krupp et al., 2004; Thomas et al., 2004; Vasyliunas, 1983).

It is generally considered that the magnetic reconnection in the Vasyliūnas cycle takes place in the nightside magnetosphere (e.g., Vasyliūnas, 1983; Bagenal et al., 2017) and is suspended at the dayside magnetodisk due to

the restriction of the magnetopause formed under the solar wind compression (e.g., Kivelson & Southwood, 2005; Palmaerts et al., 2017). It is generally believed that the magnetodisk reconnection in Vasyliūnas cycle begins to be triggered in the pre-midnight local time (LT) sector and is terminated in the predawn LT sector as it corotates with the magnetosphere. Plasma loaded from Io into the magnetodisk will be expelled using this process (Kivelson & Southwood, 2005). Theoretically, the losses of plasma in the magnetospheric Vasyliūnas cycle and the supply of plasma from Io should balance on average, approaching a quasi-equilibrium or steady state condition. However, the observed results show that the mass loss rate of plasma released by magnetotail reconnection and plasmoids is less than Io's contribution (Bagenal, 2007; Vogt et al., 2014). Such inconsistency also arises at Saturn. Recent research on Jovian magnetodisk reconnection within the magnetosphere mainly focuses on the night side (e.g., Vogt et al., 2010, 2019, 2020). The energization process of particles inside the dayside magnetosphere is still controversial.

Previous studies on Saturn's magnetic reconnection revealed that the magnetic reconnection process is critical at the dayside magnetodisk of the giant planets. Delamere et al. (2015) predicted that small-scale magnetic reconnection sites must exist inside Saturn's dayside magnetosphere based on a statistical analysis of magnetic flux circulation. Yao, Coates, et al. (2017); Yao, Grodent, et al. (2017) found a corotational reconnection site driven by an internal source in Saturn's magnetosphere that can produce Fermi acceleration of electrons. Guo, Yao, Sergis, et al., 2018, Guo, Yao, Wei, et al., 2018 subsequently discovered direct evidence of the reconnection diffusion region within Saturn's dayside magnetodisk and detailed the particle energization features using data from the Cassini spacecraft. Furthermore, Guo et al. (2019) proposed a new picture of the magnetodisk reconnection that small reconnection sites are discretely distributed in every LT sector and rotate with Saturn's magnetosphere. The magnetosphere of Saturn is relatively similar to that of Jupiter in that an internal plasma source and rapid rotation play crucial roles in magnetospheric dynamics. Based on these findings, it is expected that the dayside magnetodisk reconnection also exists in Jupiter's dayside magnetosphere and therefore warrants a detailed investigation.

In this paper, we examine magnetic field data from five spacecraft, that is, Galileo, Pioneer 10, Pioneer 11, Voyager 1, and Voyager 2, to isolate reconnection signatures when their orbits pass through Jupiter's dayside magnetosphere. We identify 18 dayside magnetic reconnection events recorded by Galileo and Voyager 2, and do not find reconnection signals from the other three spacecraft. Using data from MAG instruments (Magnetometer) from Voyager 2 (Ness et al., 1979) and MAG instruments (Magnetometer), EPD instruments (Energetic Particles Detector), and PLS instruments (Plasma Subsystem) from Galileo (Frank et al., 1992; Kivelson et al., 1992; Williams et al., 1992), a statistical analysis is performed on these dayside events to compare their signatures with those of nightside reconnection events. In Section 2, we introduce the selection criteria for screening reconnection signals and show several examples of dayside magnetic reconnection events. In Section 3, we compare the distribution, energy spectra, and characteristic energy of electrons and ions in the magnetodisk reconnection region at the dayside and the nightside. We summarize and discuss the results in Section 4.

2. Dayside Magnetodisk Reconnection Event Identified at Jupiter

In the Jovian magnetosphere, the positive direction of the north-south component of the magnetic field near the equatorial plane mainly points south. The most promising mechanism able to largely change the direction of the south component to northward near the equatorial plane is magnetic reconnection. The analysis of magnetic reconnection is often conducted in the spherical coordinate system for the convenience of demonstrating reconnection features. In this study, the spherical coordinate system, RTP (Radius-Theta-Phi) coordinates, is carried out under the right-hand Jupiter System III system. The r-axis radially points from the center of Jupiter to the spacecraft, the φ-axis is azimuthally parallel to the Jovigraphic equator and points eastward, and the θ-axis completes the right-handed system (pointing southward at the equator). The magnetic component B_θ is southward ($B_\theta > 0$) in the low and middle latitudes of the Jovian magnetosphere when there is a lack of reconnection sites. A distinct negative B_θ signature or a rapid increase in positive B_θ usually indicates a reconnection event (Guo, Yao, Sergis, et al., 2019; Guo, Yao, Wei, et al., 2018; Guo & Yao, 2024; Hones, 1976, 1977; Vogt et al., 2010, 2014; Yao, Coates, et al., 2017; Yao, Grodent, et al., 2017), including its products, that is, flux ropes, plasmoids, and dipolarization fronts.

The changes in magnetic configuration caused by magnetic reconnection and its products, as well as the high-energy particles they accelerate or carry, can affect the dynamic process of the dayside magnetosphere.

Therefore, it is important to confirm the existence of a magnetic reconnection event in the dayside magnetodisk. The triggering location of an event cannot be determined by the measurement from a single spacecraft, so it may be triggered on the dayside or may be generated elsewhere and rotate to the dayside (similar to the rotational magnetodisk reconnection on Saturn (Guo et al., 2019; Yao, Coates, et al., 2017; Yao, Grodent, et al., 2017), it can be long-lasting and evolve during the rotation. No matter where it is triggered, it will eventually affect the dayside magnetosphere. In addition, the scarcity of the spacecraft data at the dayside and the low resolution of the data did not allow us to analyze each event in depth, so we did not distinguish between ongoing magnetic reconnection and the products of magnetic reconnection in the statistical analysis.

To identify magnetic reconnection signals in the Jovian dayside magnetodisk, we surveyed magnetic field data in the Jovian magnetosphere within a region defined in local time (LT) from 06 LT to 18 LT (0, 6, 12, 18 LTs represent midnight, morning, noon and afternoon, respectively) and in radius from 30 R_J to 60 R_J inside the magnetosphere. To avoid potential confusion due to limited data resolution, we do not use data with a sampling rate always greater than 60 s. After a preliminary data screening, we obtained $\sim$600 hr of magnetic field data from the Galileo Magnetometer (MAG) instrument (Kivelson et al., 1992) and the Voyager 2 Magnetometer (MAG) instrument (Ness et al., 1979), which can be used for the search of reconnection signals. The identification criteria in this paper for reconnection events are similar to those applied by Vogt et al. (2010, 2020), while some criteria were relaxed considering the small amount of magnetic field data on Jupiter dayside. Small northward deflection of B_θ can be caused by the current sheet flapping (Jackman et al., 2009; Khurana, 1997; Nakagawa et al., 1989). To exclude the flapping structure, only strong northward deflection of B_θ (<-2 nT) was selected (Vogt et al., 2010). The selection of reconnection events follows these criteria: 1) B_θ is negative and has values less than -2 nT; or 2) when positive, B_θ is larger than 3 nT and two or more times larger than the background B_θ value (denoted $\overline{B_\theta}$) for at least 1 min, where $\overline{B_\theta}$ is defined as the 10-hr running average of $|B_\theta|$. We require that the duration of the reconnection event be longer than 1 min. The duration of the event is the period that B_θ remains negative or B_θ is at least 1.5 times the background levels. Two signals that are separated by more than 1 hr are treated as two events. Through the above criteria and further artificial inspection, we could identify the reconnection events in the Jovian dayside magnetodisk and obtain the duration of these events.

Using these criteria, we identified 18 dayside magnetodisk reconnection events. All dayside magnetodisk reconnection events and their information (duration, location, inside/outside the plasma sheet, etc.) are listed in Table 1. In the following subsections, several examples of dayside magnetodisk reconnection events in the morning (06:00-10:00 LT) sector, noon (10:00-14:00 LT) sector, and afternoon (14:00-18:00 LT) sector are shown in Figures 1–3.

2.1. Dayside Reconnection Event Examples: Morning Sector

Figure 1 shows two magnetic reconnection events (highlighted by orange shaded area) in the morning sector ($\sim$06:00-07:00 LT), Event 3 and Event 4 in Table 1, respectively. Figures 1a–1c show three components of the magnetic field B_r (magenta), B_φ (blue), B_θ (red) in the RTP coordinate system and the magnitude of the average magnetic field components B_{tot} (black). Figure 1b clearly shows short episodes of B_θ reversals. The horizontal green lines in Figure 1b present the background field $\overline{B_\theta}$ and the value of -2 nT. For Event 3, B_θ turned from positive (6.43 nT) to negative (-2.58 nT). For Event 4, B_θ turned from negative (-3.96 nT) to positive (6.54 nT). At the same time, the B_r component in Event 3 was distinctly increased but was slightly decreased in Event 4; the B_φ components in Event 3 and Event 4 were both distinctly increased.

To identify whether the spacecraft crosses the magnetic diffusion region, Figures 1d and 1e describe the magnetic vector in the X-line coordinates. The X-line coordinate system is a current sheet coordinate system that removes the bend-back effect (Arridge et al., 2016), which has been successfully applied to Saturn (Arridge et al., 2016; Guo, Yao, Sergis, et al., 2018, Guo, Yao, Wei, et al., 2018) and Jupiter's magnetodisk (Guo, Yao, Dunn, et al., 2021; Guo, Yao, Grodent, et al., 2021). In the X-line coordinate system, during the crossing of a magnetic reconnection diffusion region by a spacecraft, when the recorded B_x is positive, the Hall magnetic component B_y and the normal component B_z have the same polarity (both positive or negative), and when B_x is negative, B_y and B_z have opposite polarity (if one is positive then the other is negative). For Event 3, B_x is negative, and B_y has a sign generally opposite to B_z; for Event 4, B_x is positive, and B_y has a sign generally similar to B_z. The magnetic signatures are in accordance with the Hall reconnection picture.

Table 1
Detail Information of Magnetic Reconnection Events in Jupiter's Dayside Magnetodisk Encountered by Galileo and Voyager-2 Spacecraft

Event (#)	Start time (UT)	End time (UT)	Duration (mins)	Local time (hrs)	Distance (R_J)	Plasma sheet (Out/in)	Catalog Sector	Spacecraft	B_θ signature
1	1996-06-23T16:14	1996-06-23T17:36	82	6.83	47.52	In	Morning	Galileo	bipolar
2	1996-06-23T20:18	1996-06-23T22:18	120	6.88	46.03	In	Morning	Galileo	bipolar
3	1996-06-24T01:14	1996-06-24T01:38	24	6.97	44.62	Out	Morning	Galileo	bipolar
4	1996-11-02T18:54	1996-11-02T19:29	35	6.42	40.77	Out	Morning	Galileo	bipolar
5	1996-11-02T22:26	1996-11-02T23:30	64	6.50	39.59	In	Morning	Galileo	positive
6	1996-11-03T01:57	1996-11-03T04:28	151	6.60	38.24	In	Morning	Galileo	positive
7	1996-12-15T03:11	1996-12-15T04:02	51	6.18	41.94	In	Morning	Galileo	positive
8	2002-01-20T08:58	2002-01-20T16:33	455	12.42	39.48	Out and in	Noon	Galileo	bipolar
9	2002-01-20T20:01	2002-01-21T04:06	485	12.59	44.01	Out and in	Noon	Galileo	bipolar
10	2002-01-21T11:10	2002-01-21T12:15	65	12.74	48.47	In	Noon	Galileo	bipolar
11	1979-07-07T07:34	1979-07-07T09:35	121	11.06	41.71	Out	Noon	Voyager 2	bipolar
12	1979-07-07T18:33	1979-07-07T19:41	68	11.34	35.85	Out	Noon	Voyager 2	bipolar
13	2000-05-23T12:22	2000-05-23T13:11	49	15.92	33.24	In	Afternoon	Galileo	bipolar
14	2000-05-25T03:04	2000-05-25T03:24	20	16.59	48.39	Out	Afternoon	Galileo	positive
15	2000-05-25T11:17	2000-05-25T11:45	28	16.68	51.34	Out	Afternoon	Galileo	negative
16	2000-05-25T18:48	2000-05-25T20:03	75	16.77	54.07	In	Afternoon	Galileo	bipolar
17	2000-05-26T10:36	2000-05-26T10:39	3	16.91	59.13	In	Afternoon	Galileo	negative
18	2002-11-03T10:02	2002-11-03T10:31	29	15.47	31.95	In	Afternoon	Galileo	bipolar

In addition, during the periods of Events 3 and 4, the differential number flux of EPD energetic particles (electrons, all ions, H^+, O^{n+}, and S^{n+}) are all enhanced. The count rate of PLS low-energy ions is significantly enhanced in Event 4 and slightly enhanced in Event 3. A remarkable feature in the energetic ion flux (Figure 1g) is that the fluxes of the ions with ∼100 keV (blue and cyan curves) are comparable and even larger than those with ∼40 keV (black and purple curves). These enhancement features reveal that the particles have undergone some kind of acceleration or heating process. Combining characteristics of the Hall magnetic field and particle energization, we suggest that the spacecraft crosses two ongoing magnetic reconnection diffusion regions.

2.2. Dayside Reconnection Event Examples: Noon Sector

Several magnetic reconnection events in the noon sector (∼11:00-13:00 LT) are shown as marked by the orange shaded area in Figure 2. Figures 2a–2d show three noon-sector events identified from Galileo MAG data. Figures 2e–2h show a noon-sector event identified from Voyager 2 MAG data. The count rate data of low-energy ions in Figure 2d were obtained from the Galileo Plasma Subsystem (PLS) instrument, and the differential energy flux data of low-energy electrons in Figure 2h were obtained from Voyager 2 Low-Energy Charged Particle investigation (LECP) (Krimigis et al., 1977).

In Figure 2b, the magnitude of B_θ in Event 8 and Event 9 changes from positive to negative values several times over a long period. The B_θ signals between the two gray vertical dotted lines in Events 8 and 9 have some similarities, which might be evolving reconnection sites rotating around Jupiter and encountering the spacecraft twice, similar to the rotating reconnection picture discovered in the Saturnian magnetodisk by Yao, Coates, et al. (2017) ; Yao, Grodent, et al. (2017) and Guo et al. (2019). Event 12 in Figures 2e–2h starts at a positive value, decreases to a maximum negative value (−1.50 nT), and finally becomes positive again (larger than two times $\overline{B_\theta}$). The integral flux of energetic electrons in Figure 2h is increased.

The gray vertical solid lines in Figures 2e–2h represent the moment that the spacecraft passes through the plasma sheet center. Therefore, Event 12 occurs outside the plasma sheet. Event 8 and Event 9 span outside and inside the plasma sheet because they have a very long duration. Because the intensity of particle energy flux inside the
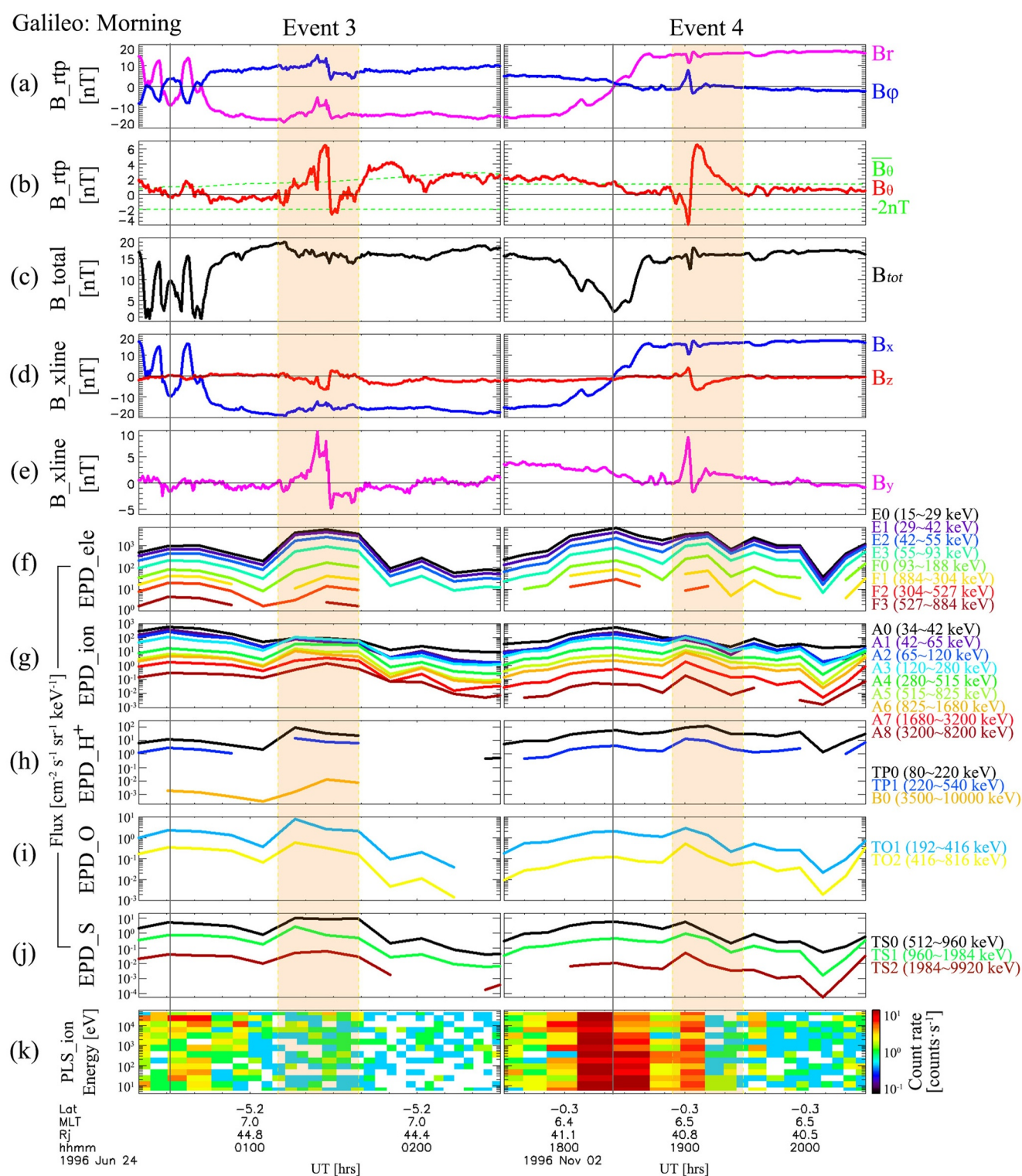
Figure 1. Two examples of magnetic reconnection events identified from the Galileo observations in the morning sector (∼06:00-07:00 LT) within the Jovian magnetodisk. (a–b) Three components of magnetic field B_r (magenta), B_φ (blue), and B_θ (red) in the RTP (Radius-Theta-Phi) coordinate system. (c) Average magnetic field component B_{tot} (black). (d–e) Three components of magnetic field B_x (blue), B_y (magenta), and B_z (red) in the X-line coordinate system. (f–j) The differential flux data of various particle species (electrons, all ions, H^+, O^{n+}, and S^{n+}) with various energy channels. (k) The count rate of ions with various lower energy channels. The orange-shaded area shows the period of the reconnection event, and the vertical solid gray line indicates the center of the plasma sheet.
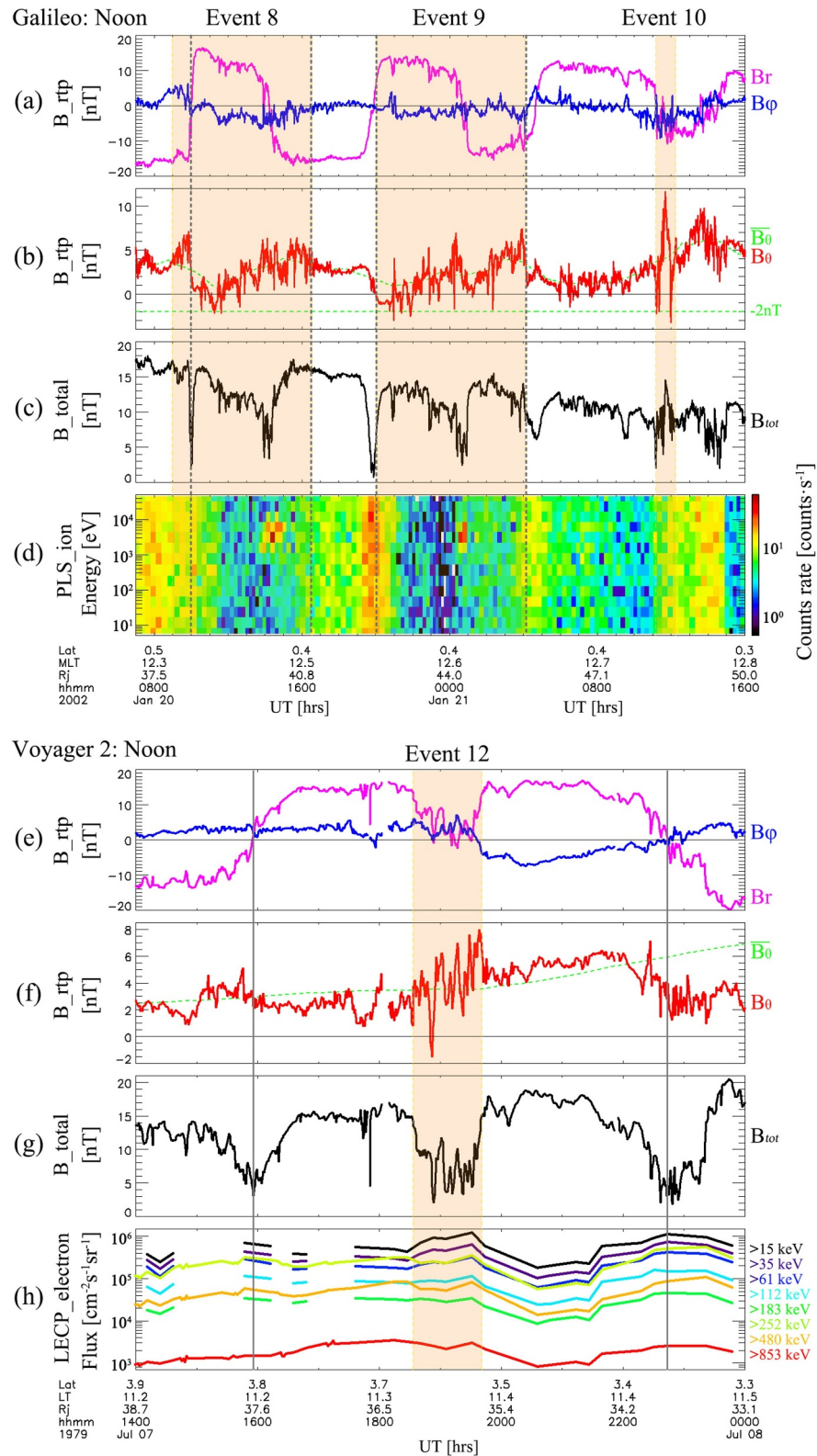
Figure 2. Several examples of magnetic reconnection events near the noon sector (∼11:00-12:00 LT) in Jovian magnetodisk. (a–c, and e–g) The magnetic field B_r (magenta), B_φ (blue), B_θ (red), and B_{tot} (black). (d) The ion lower energy spectrum from Galileo PLS data. (h) The electron energy spectrum from Voyager 2 LECP data. The orange-shaded areas show the period of the reconnection event. The vertical gray dotted lines in panels (a–d) mark two similar B_θ signals, and the vertical gray solid lines in panels (e–h) indicate the center of the plasma sheet.
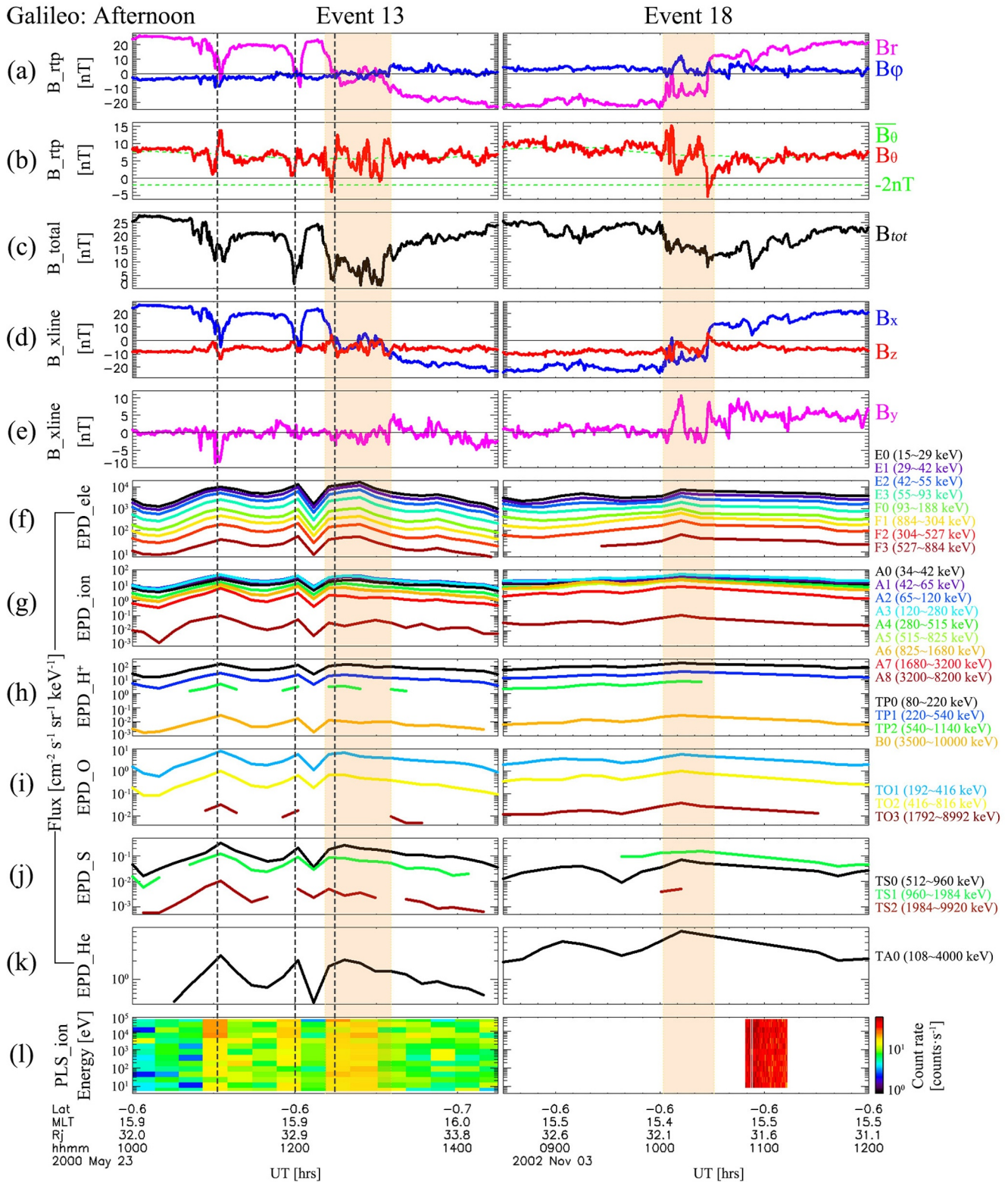
Figure 3.

plasma sheet is generally stronger than that outside the plasma sheet, the energization features of the magnetic reconnection inside and outside the plasma sheet should be analyzed separately. Therefore, as shown in the following Sections 3.2 and 3.3, the reconnection events are divided into groups inside and outside the plasma sheet.

2.3. Dayside Reconnection Event Examples: Afternoon Sector

Figure 3 shows two magnetic reconnection events in the afternoon sector (∼15:00-16:00 LT) as marked by the orange-shaded areas. There are three potential flux ropes that exist in Event 13 as marked by the three dashed vertical lines. The B_θ components marked by the first and third vertical lines show bipolar signatures while the strengths of the B_φ component are enhanced, indicating a helical magnetic structure with a strong core field. The center of the second B_θ bipolar signature corresponds to a weak B_φ value, indicating that the structure is close to a loop-like configuration. The fluxes of the energetic particles (Figures 3f–3k) and hot ions (Figure 3l) are all increased at the three structures. Despite the first and second flux ropes do not meet the criteria of lasting at least 1 min, the significant bipolar signatures and the high flux of energetic particles indicate they are the product of the magnetic reconnection. According to the variation of the B_r component, the spacecraft should be out of the current sheet before the orange shaded duration, and the spacecraft should not cross the flux rope center to record a much stronger signature. After the third vertical line, the B_θ component varies quickly and could also be related to flux ropes or dipolarization fronts; however, it is hard to identify them with such a low data resolution.

The negative B_θ in Event 18 seems to correspond to a reconnection diffusion region for which the enhancement of the B_y component is consistent with the Hall magnetic field. The B_x component is positive when B_z is positive, so the sign of the Hall magnetic component B_y should be positive. Before the negative B_θ, the enhancement of the B_θ component accompanied by a decrease in B_r strength indicates a dipolarization front (Yao, Coates, et al., 2017; Yao, Grodent, et al., 2017) on the planetary side of the X-line (the side closer to the planet). B_y enhances positively near the dipolarization front, which is also consistent with the positive Hall magnetic component when B_x and B_z are negative. The particles are energized in this event, as shown in Figures 3f–3k.

3. Statistical Properties of Magnetic Reconnection Events

3.1. Distribution

The nightside reconnection events are important comparison points in our research. We used the list of nightside events located in the 30–60 R_J range from Vogt et al. (2010), which is included in Table S1 in Supporting Information S1. Figure 4 shows the location distribution of magnetic reconnection events on the dayside and nightside in the Jupiter Solar Equatorial (JSE) coordinate system X-Y plane (Z is aligned with Jupiter's spin axis and positive northward, Y is the cross product of the vector of Z and vector of Jupiter to Sun, X completes the right-handed system). The cyan, magenta, and orange curves represent the Galileo, Voyager 1, and Voyager 2 trajectories, respectively. The diamonds with different colors indicate the locations of the dayside and nightside reconnection events identified from Galileo, Voyager 1, and Voyager 2 satellite data. As can be seen clearly from Figure 4, the dwell time that Galileo spends on Jupiter's dayside is significantly less than that on the nightside, and there is no data beyond 30 R_J at the ∼09:00-11:00 LT sector. Although the total dwell duration of Galileo within the dayside magnetodisk is short, we have identified a relatively large number of magnetic reconnection events on the dayside. The ratio of the magnetic reconnection duration to the spacecraft dwell time between 30 R_J and 60 R_J for dayside and nightside is 0.033 and 0.026, respectively. This calculation cannot precisely obtain the occurrence rate of the reconnection, but it implies that the magnetic reconnection process is frequent at the dayside magnetodisk.

The number of events at each LT sector are shown in Figure 5a. Since the satellites take more time on the nightside than on the dayside, there are significantly more events on the nightside than on the dayside. Figure 5a

Figure 3. Two examples of magnetic reconnection events identified from the Galileo observations in the afternoon sector (∼15:00-16:00 LT) within the Jovian magnetodisk. (a–b) Three components of the magnetic field B_r (magenta), B_φ (blue), and B_θ (red) in the RTP coordinate system. (c) Average magnetic field component B_{tot} (black). (d–e) Three components of magnetic field B_x (blue), B_y (magenta), and B_z (red) in the X-line coordinate system. (f–k) The differential flux data of various particle species (electrons, all ions, H^+, O^{n+}, S^{n+}, and He) with various energy channels. (l) The count rate of ions with various lower energy channels. The orange-shaded area shows the period of the reconnection event, and the vertical dotted black lines indicate three potential flux ropes.
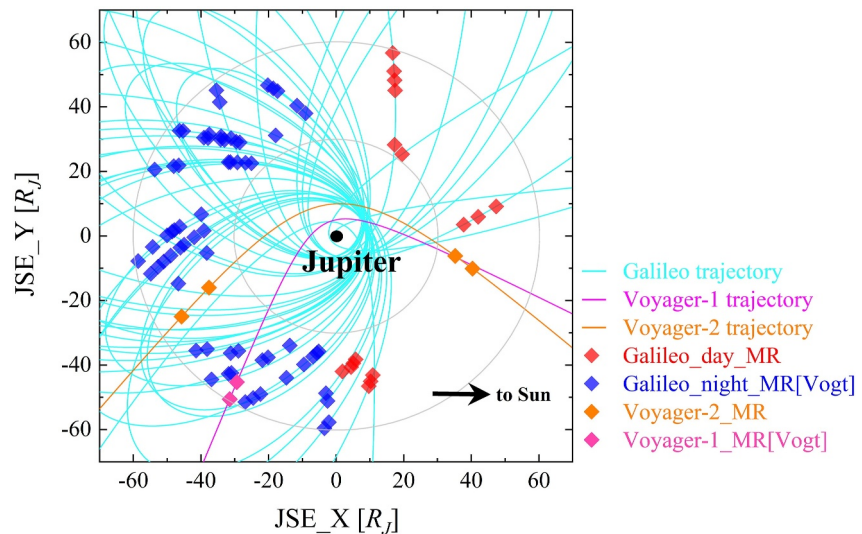
Figure 4. Locations of magnetic reconnection (MR) events identified by Galileo, Voyager 1, and Voyager 2 are shown here in the X-Y plane of the Jupiter Solar Equatorial (JSE) coordinate system (the Z is aligned with Jupiter's spin axis and positive northward, Y is the cross product of the vector of Z and vector of Jupiter to Sun, X completes the right-handed coordinate system). Galileo, Voyager 1, and Voyager 2 orbits are shown in cyan, magenta, and orange curves. The dayside events are shown in red (identified from Galileo) and orange (identified from Voyager 2). The nightside events are shown in blue (identified from Galileo), pink (identified from Voyager 1), and orange (identified from Voyager 2).

suggests that magnetic reconnection occurs more often in the sector regions of 21:00-22:00 LT, 00:00-01:00 LT, and 03:00-07:00 LT on the nightside. Vogt et al. (2010) also show a similar result between 30 R_J and 60 R_J in their Figure 9. We cannot determine the LT dependence of the dayside events because of the lack of orbits across many LT sectors. Figure 5b shows the dependence between the number of events and their radial distance from Jupiter. On the nightside, a relatively large number of events are distributed between 45 R_J and 55 R_J. However, on the dayside, the distribution of event numbers within 30–60 R_J is similar to a Gaussian distribution with a peak between 40 and 45 R_J. However, due to the small number of spacecraft orbits on the dayside, the above distribution characteristics need to be further confirmed. Figure 5c shows the distribution of the observed duration of reconnection events. The durations of the relatively large number of dayside and nightside events are typically in the range of 20–80 min. Nonetheless, some events have a duration of more than 320 min on both the dayside and nightside.

Figures 6a and 6b show 2D histograms of the reconnection event occurrence rate (color levels) with LT (*x*-axis in both plots), radial distance (*y*-axis in plot a), and event duration (*y*-axis in plot b). The occurrence rate is calculated as the ratio between the number of reconnection events within a given bin and the total number of events. The local time in Figure 6 is divided into six sectors: 06:00-10:00, 10:00-14:00, 14:00-18:00 LT on the dayside, and 18:00-22:00, 22:00-02:00, 02:00-06:00 LT on the nightside. The color bar is the occurrence rate of events, and the areas without data are filled with gray. Figure 6a suggests that the occurrence rate increases from dusk to dawn along with Jupiter's rotational direction, and also increases with radial distance. More data is needed to uncover the dependencies on the dayside. Figure 6b shows that the dayside and nightside events with extremely long durations (duration greater than 320 min) are mainly found in the noon and morning sectors, respectively. The nightside events with less than 100 min of duration are almost uniformly distributed at each LT and peak at pre-evening.

3.2. Energy Spectrum

In this section, we classified all events by their location either inside or outside the plasma sheet, and either on the dayside or nightside, and compared differences in the particle energy spectrum for electrons and ions. As a result, we obtained four data sets for each particle species, that is, the dayside reconnection cases inside and outside the plasma sheet and the nightside reconnection cases inside and outside the plasma sheet. The classification process of whether an event is inside or outside the plasma sheet is performed manually. The periodic changes in the sign
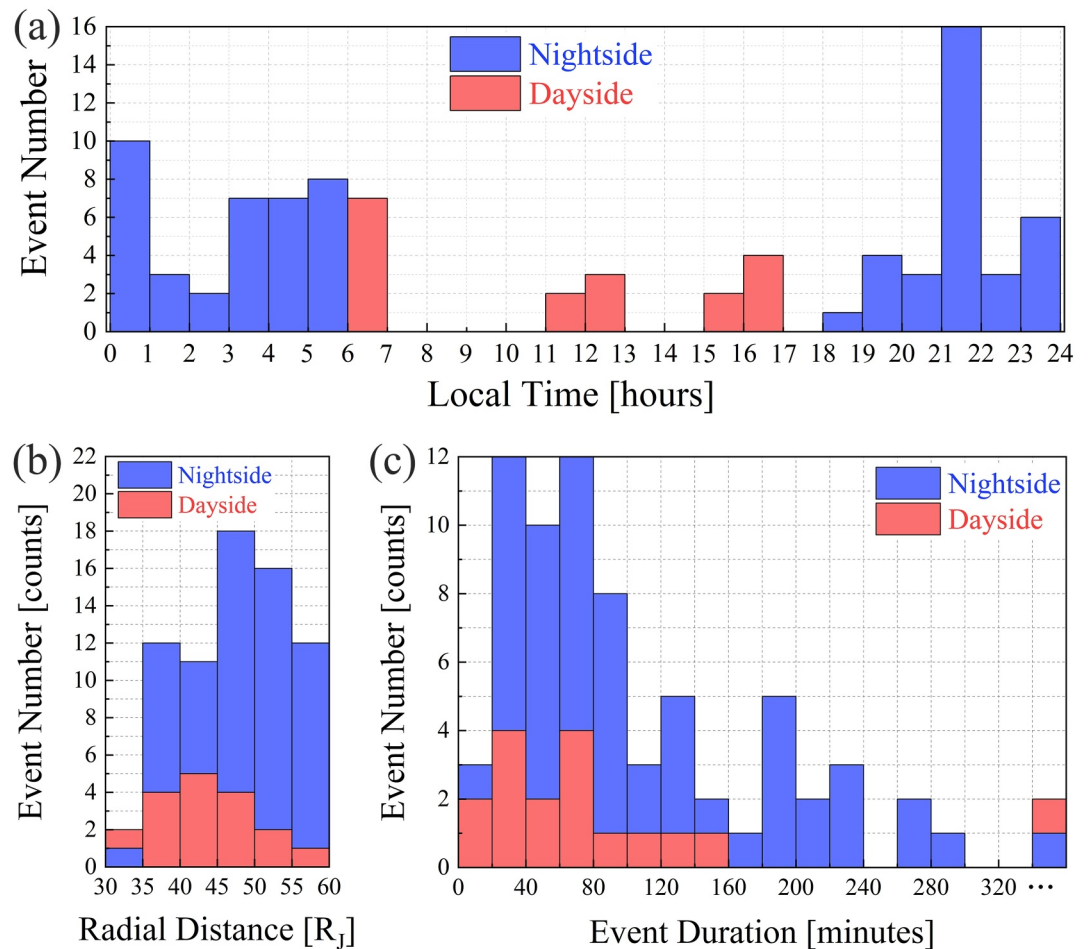
Figure 5. Histograms of all dayside (red) and nightside (blue) magnetic reconnection events, with bins in panel (a) each local time hour, (b) every five R_J radial distances to Jupiter, and (c) every 20 minutes duration.

of the radial component of the magnetic field B_r (such as the magenta line in Figure 2a) indicate that the plasma sheet moved either upwards or downwards through the spacecraft (Kivelson, 2015). At the same time, the average magnetic field magnitude B_{tot} measured by the spacecraft always decreases abruptly, as shown in Figures 2c and 2g. Therefore, when the identified reconnection signal spans the duration when B_r changes sign and when B_{tot} is abruptly decreased, this reconnection event is classified as an event inside the plasma sheet; otherwise, it is classified as an event outside the plasma sheet. For extremely long-duration events, they are split into several parts according to the above classification criteria.

We divide the data set by two radial distance ranges (30–45 R_J and 45–60 R_J) and four local time ranges (06–12 LT and 12–18 LT for dayside, 18–24 LT and 00–06 LT for nightside). We take a geometric average of the electron and ion differential number fluxes for all reconnection events and non-reconnection duration (i.e., the duration not meeting the criteria in Section 2) in each data set. In Figure 7, the results for reconnection and non-reconnection are presented by the solid lines (joining data points) and dotted lines, respectively. In the 30–45 R_J range, the energetic particle fluxes at the dayside are comparable to or even larger than that at the nightside. In the 45–60 R_J range, the fluxes in the morning sector are larger than nightside and the fluxes at the energies of tens of keV in the afternoon sector are smaller than nightside. The magnetodisk experiences compression in the morning sector and quick expansion in the afternoon sector (Kivelson & Southwood, 2005), which may lead to the difference in the energetic particle flux between the 30–45 R_J and 45–60 R_J regions. Many events are products of the magnetic reconnection process and their size can be modified during the compression and expansion of the magnetodisk.
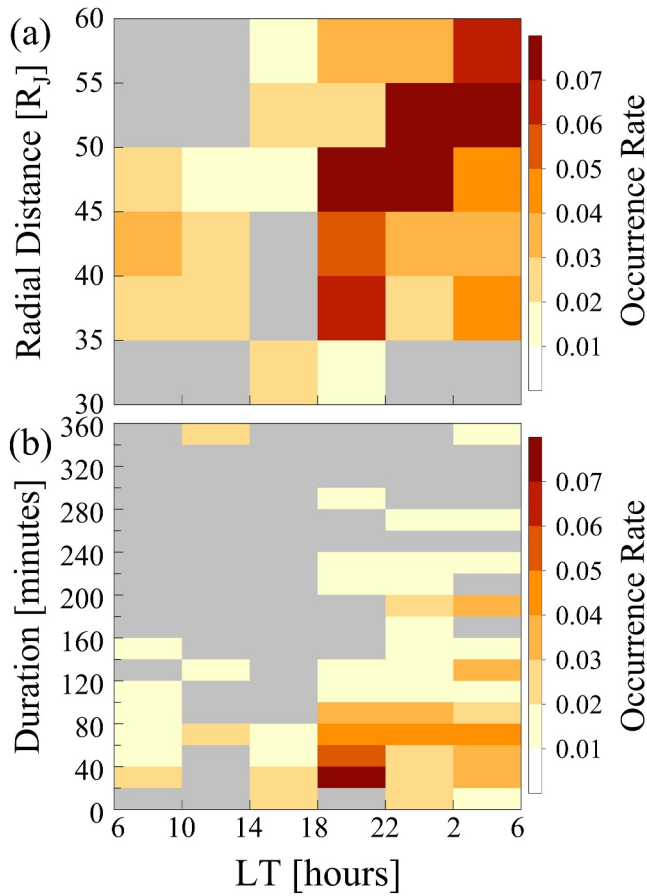
Figure 6. The 2D histograms show the occurrence of reconnection events within bins defined by: (a) local time and radial distance and (b) local time and event duration, respectively. Every 4 hours of local time is divided into a sector. The areas without data are filled with gray.

At dayside, the fluxes during the magnetic reconnection events are higher or comparable to those during non-reconnection durations both inside and outside the plasma sheet. At nightside, especially for the sector of 00–06 LT, the fluxes of reconnection events in the 30–45 R_J range are smaller than the non-reconnection duration, while the fluxes of reconnection events in the 45–60 R_J range are larger than or comparable to the non-reconnection duration. The ratio between the fluxes observed during reconnection and the non-reconnection duration can be found in Figure S1 in Supporting Information S1. Noting that not all the events are the ongoing reconnection diffusion region, the flux could have evolved during the long-distance transportation and rotation of the structure in the nightside current sheet. The flux difference at different distances might be related to the field-aligned current system; however, this paper will focus on the dayside magnetodisk reconnection and the evolution in nightside will be settled in the future study.

The electron and ion energy spectra both appear to have a power law distribution with a negative exponent. This is consistent with the result of Liu et al. (2021) that in Jupiter's magnetosphere, the energy spectrum of both electrons and protons at different radial distances can be well-fitted by power laws. In Figure 7, the energy spectra are fitted using linear fitting y = a + bx. The decrease in the slope of the particle energy spectrum, also known as the energy spectral index, generally indicates that the particle is energized (Blöcker et al., 2022; Kronberg & Daly, 2013). The spectral slopes of the dayside reconnection are smaller than or comparable to those of the non-reconnection. At nightside, the relation between reconnection events and non-reconnection duration depends on the distance to Jupiter, indicating that the evolution in the uncompressed nightside magnetodisk is more complex than that in dayside. The limitation of the small dayside data set prevents us from conducting more in-depth research. Nevertheless, we can at least confirm that the dayside magnetodisk reconnection process can provide non-negligible flux of energetic particles into the magnetosphere and cannot be ignored in Jupiter's magnetospheric dynamics.

3.3. Characteristic Energy

In order to characterize the energetic particles during the period of reconnection events on dayside and nightside, we calculated the characteristic energy E_c and energy flux I_E (Clark et al., 2018; Mauk et al., 2004):

$$E_c = \frac{\int_{E_{\min}}^{E_{\max}} J \cdot E \mathrm{d}E}{\int_{E_{\min}}^{E_{\max}} J \mathrm{d}E} \text{ (in units of keV),}$$

where J is the particle differential number flux in units of $\mathrm{cm}^{-2}\,\mathrm{sr}^{-1}\,\mathrm{s}^{-1}\,\mathrm{keV}^{-1}$, $E_{\min}$ and $E_{\max}$ are the lower and upper energy limits for the EPD instruments (15 and 884 keV for electrons, and 34 and 8,200 keV for ions, respectively), and E is the central energy of each energy channel. The numerator in the above equation is the integral energy flux $I_E = \int_{E_{\min}}^{E_{\max}} J \cdot E \mathrm{d}E$.

Figure 8 shows the characteristic energy of energetic electrons/ions as a function of the energy flux on the dayside/nightside reconnection inside (Figures 8a and 8b) and outside the plasma sheet (Figures 8c and 8d). The vertical solid lines in all panels represent the average of characteristic energy, and the horizontal dotted lines represent the average of energy flux. The results for different local time ranges are presented in different colors. The electrons have an average characteristic energy of around 100 keV both inside and outside the plasma sheet both on the dayside and nightside. The average characteristic energy of ions is 7–10 (3–5) times larger than that of electrons at dayside (nightside). The dayside energy fluxes are comparable to and even slightly larger than the nightside energy fluxes, indicating that the dayside magnetodisk reconnection has a comparable ability to power
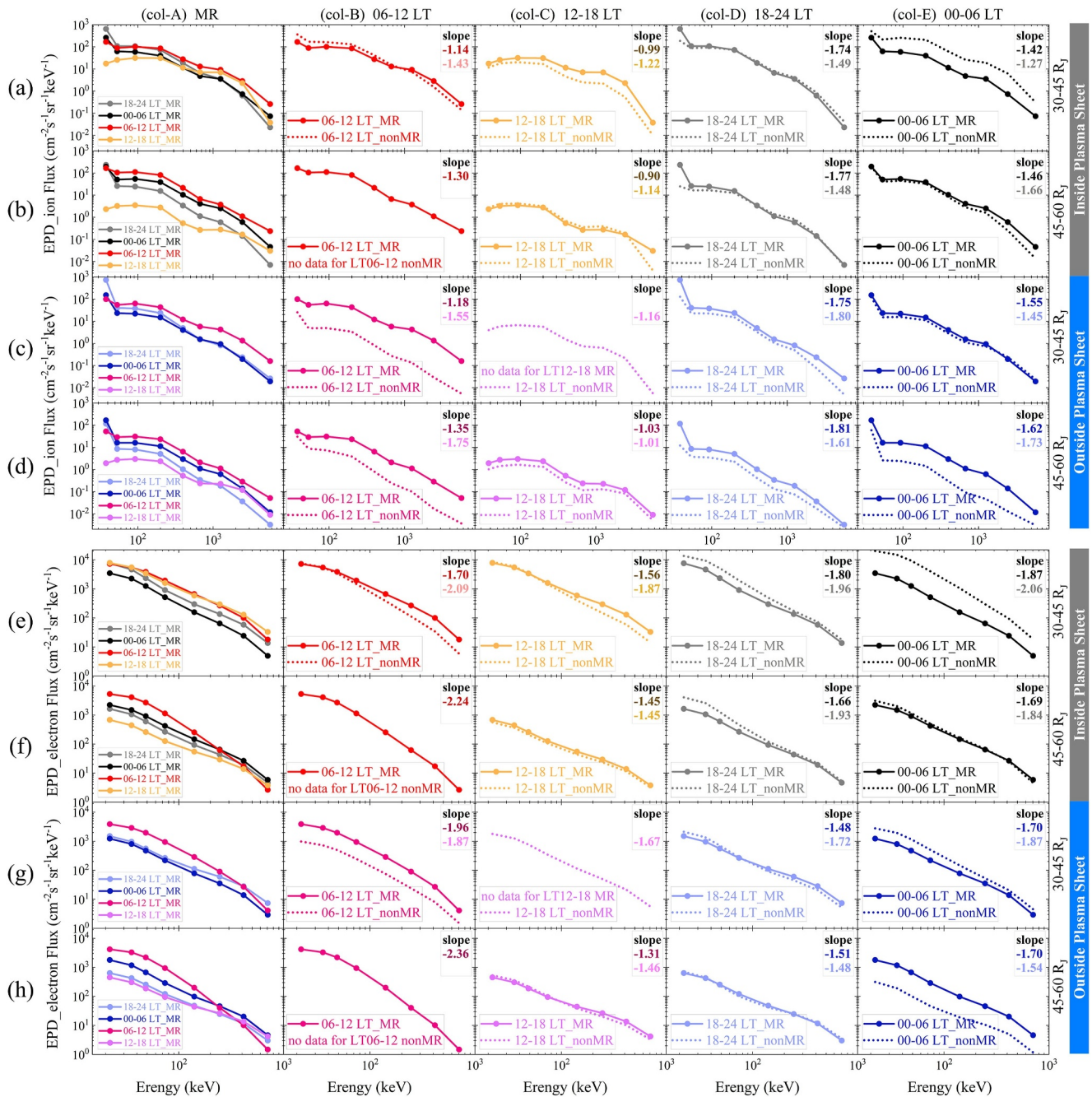
Figure 7. The energy spectra of Galileo EPD ions (a–d) and electrons (e–h) corresponding to the magnetic reconnection (MR, solid lines with dots) and non-reconnection (nonMR, dotted lines) events in the following two conditions: inside (a–b, and e–f) and outside (c–d, and g–h) the plasma sheet. The data set is divided into radial distance ranges of 30–45 R_J and 45–60 R_J. The results for the different local time ranges of dayside and nightside are distinguished by different colors. The slope is the result of a simple linear fit $y = a + bx$.

the magnetosphere as the nightside reconnection. Though the electron characteristic energy is low, the electron energy flux has a value similar to the ion energy flux, which may be caused by a larger differential flux for the electrons than the ions, as shown in Figure 7. It should be noted that the calculations are only performed for the energy ranges from 15 to 884 keV for the electrons and 34 to 8,200 keV for the ions. Nonetheless, the high-energy particles observed by the EPD instruments have a significant impact on the magnetosphere-ionosphere coupling process. The characteristic energies of ions outside the plasma sheet are comparable to those inside the plasma sheet, implying that the energized ions can travel into high magnetic latitudes.
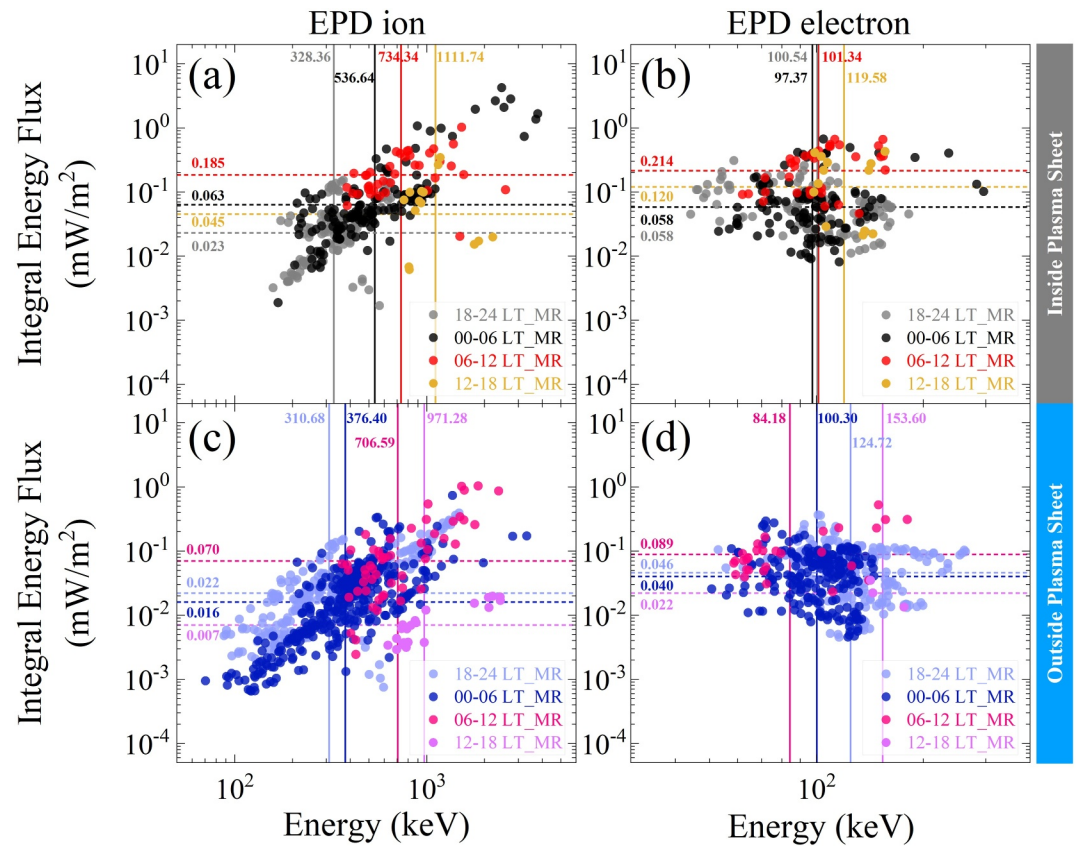
Figure 8. The relationship between the characteristic energy and energy flux of energetic ions (a), (c) and electrons (b), (d) during the dayside and nightside reconnection event periods. Different colors represent different local time ranges. (a–b) Inside the plasma sheet; (c–d) outside the plasma sheet. The vertical solid lines in all panels represent the geometric average value of characteristic energy, and the horizontal dotted lines represent the geometric average value of energy flux.

We have only 3 cases around the noon sector, and the values averaged over all the dayside events mix the features in a large range of local times. To analyze the local time dependency, Figure 9 shows the distribution of the mean characteristic energies (Figures 9a, 9b, 9e, and 9f) and mean energy fluxes (Figures 9c, 9d, 9g, and 9h) of the electrons/ions in reconnection events in the JSE X-Y plane. The value in each $10\,R_J \times 10\,R_J$ bin is calculated from the average of all events located in this square. The characteristic energy of the ions is low around the midnight sector and high in the dawn and afternoon sectors. The ion characteristic energy around the noon sector is higher than at midnight if the three cases at noon observed by Galileo are indeed representative. The characteristic energy distribution of the electrons has no obvious local time dependency. The energy fluxes of both electrons and ions show distinct high values at the dawn sector, which could be consistent with the frequently occurring auroral dawn storm (Bonfond et al., 2021; Grodent, 2015; Yao et al., 2020). The energy fluxes around the noon sector are non-negligible compared to the nightside at distances similar to Jupiter ($>40\,R_J$). In conclusion, the magnetodisk reconnection process at Jupiter has a comparable effect on the particle acceleration at all LTs.

4. Summary and Discussion

Recent studies have reported many magnetic reconnection events occurring in Saturn's dayside magnetosphere, suggesting that the compression of the solar wind onto the magnetosphere cannot wholly suppress the magnetic reconnection process at the dayside magnetodisk. Like Saturn, Jupiter, which is rapidly rotating and contains an internal plasma source, can exhibit dayside magnetodisk reconnection. Yao et al. (2020) revealed a recurrent magnetic dipolarization event after one planetary rotation, implying the potential corotating magnetic dipolarization at Jupiter, while the direct confirmation of dayside magnetodisk dipolarization and the potentially associated magnetic reconnection was not reported in the literature that we are aware of. In this study, we have examined the magnetic field data from all spacecraft that have visited Jupiter's dayside magnetosphere and
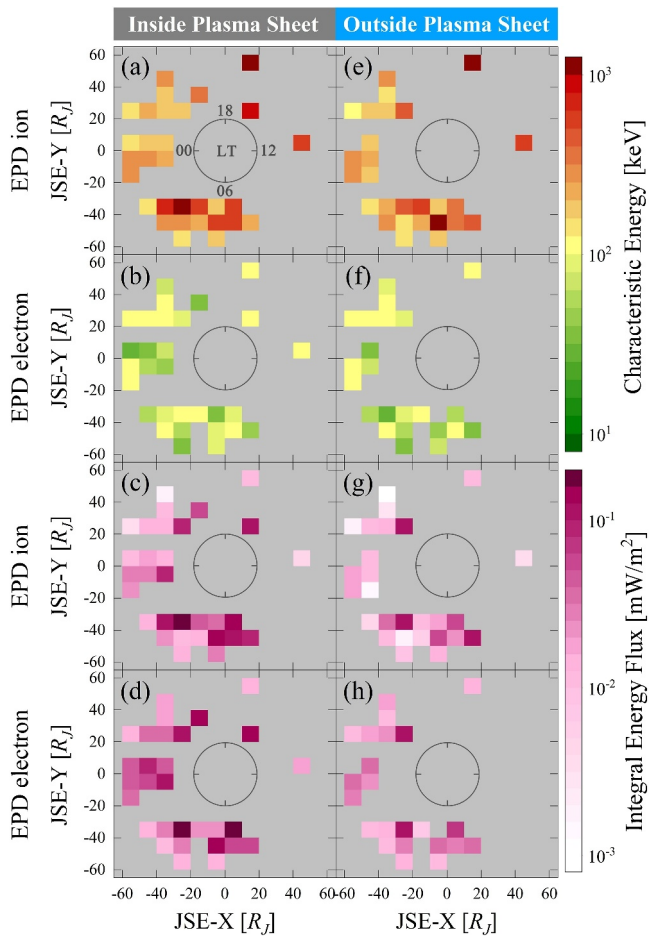
Figure 9. The geometric mean value of characteristic energy (a, b, e, f) and energy flux (c, d, g, h) for ions/electrons during reconnection events, with event locations projected to the equatorial plane of the JSE coordinate system. (a–d) Inside the plasma sheet; (e–h) outside the plasma sheet. The value in each $10 \, R_J \times 10 \, R_J$ bin is calculated from the average of all events in this square. The areas without data are filled with gray.

identified 18 dayside magnetic reconnection events from the Galileo and Voyager 2 spacecraft. Afterward, we analyzed the particle (electron and ion) flux, energy spectra, and characteristic energy of these dayside events and compared them to those of nightside magnetic reconnection. The results are summarized as follows.

- Although the observation data set is rather small and only partially covers the Jovian dayside magnetosphere, the considerable number of recorded events indicates that the occurrence rate of dayside magnetic reconnection is significant.
- The fluxes of the energetic electrons and ions in the dayside magnetodisk reconnection region are comparable to or even larger than those in the nightside reconnection region. The differential flux of the energetic particles is consistent with the day-night asymmetry in the magnetodisk.
- For the reconnection events, the characteristic energy of the ions at the dayside is higher than that in the midnight sector, while the characteristic energy distribution of the electrons has no obvious local time dependency. The energy flux is large at the dawn sector for both ions and electrons.

The statistical results in this study show the overall effects of the magnetic reconnection process at the dayside magnetodisk. The magnetic reconnection region may often be accompanied by some interesting magnetic structures, such as plasmoids, traveling compression regions (TCR), and flux ropes in a planet magnetotail (Zong et al., 2004). In this study, we do not distinguish these structures. Some events in Table 1 could be plasmoids or flux ropes, which are byproducts of magnetic reconnection and have similar negative and enhanced B_θ profiles. To confirm a reconnection diffusion region, such as the ion diffusion identified at Saturn (Guo, Yao, Wei, et al., 2018), high-resolution plasma velocity or pitch-angle information is needed, which is lacking in the data from Galileo and Voyager 2. The lack of reliable velocity data prevents us from estimating the size of the reconnection sites. The structures inside the magnetodisk could move both radially and azimuthally. The corotation speeds are 370 km/s and 750 km/s for 30 R_J and 60 R_J, respectively. If only the azimuthal length of the reconnection X-line is estimated under a corotation assumption and neglecting the spacecraft's orbital motion (roughly 10 km/s), the size of the X-line ranges from 2 R_J to 42 R_J at an average of 20 R_J. It should be noted that this estimation method is crude, and a better result requires better data or simulations in the future.

Additionally, the reconnection sites rotate with the Jovian magnetosphere, as revealed by Figures 2a–2d, which would be coherent with the rotating events observed at Saturn (Guo et al., 2019; Yao, Coates, et al., 2017; Yao, Grodent, et al., 2017). In this case, the spacecraft crossed the reconnection region roughly along the reconnection X-line; the signals could be different from those observed primarily along the outflow direction. This will bring difficulty in determining the spacecraft's trajectory in the reconnection region and distinguishing different reconnection structures. In the rotating magnetosphere, the energized particles highly likely from the rotating reconnection region can lead to rotating multiple field-aligned current systems and rotating aurorae at Saturn (Guo, Yao, Dunn, et al., 2021). The magnetic reconnection has been observed to relate to auroral enhancements in the Jovian ionosphere at the dawn sector (Guo, Yao, Grodent, et al., 2021). The rotating dayside magnetodisk reconnection sites, especially the long-duration events, can be closely related to dayside auroral emissions.

The dayside magnetodisk processes at Jupiter, including magnetic reconnection, dipolarization, and injection, shall be further investigated using numerical tools. Direct observations confirm the existence of the processes and can roughly quantify the energization and mass circulation, while obtaining a global picture is a big challenge, particularly considering the limited data set in the giant planetary system. On the other hand, the numerical simulation could provide a global picture (e.g., Zhang et al., 2021), and the combination of the ground truth data would strongly benefit the understanding of the complex giant planetary systems.

Data Availability Statement

All data used in this study were from the data set on the Planetary Data System at https://search-pdsppi.igpp.ucla.edu/search/?t=Jupiter&facet=TARGET_NAME.

References

Arridge, C. S., Eastwood, J. P., Jackman, C. M., Poh, G., Slavin, J. A., Thomsen, M. F., et al. (2016). Cassini in situ observations of long-duration magnetic reconnection in Saturn's magnetotail. *Nature Physics*, *12*(3), 268–271. https://doi.org/10.1038/NPHYS3565

Bagenal, F. (2007). The magnetosphere of Jupiter: Coupling the equator to the poles. *Journal of Atmospheric and Solar-Terrestrial Physics*, *69*(3), 387–402. https://doi.org/10.1016/j.jastp.2006.08.012

Bagenal, F., Adriani, A., Allegrini, F., Bolton, S. J., Bonfond, B., Bunce, E. J., et al. (2017). Magnetospheric science objectives of the Juno mission. *Space Science Reviews*, *213*(1–4), 219–287. https://doi.org/10.1007/s11214-014-0036-8

Blöcker, A., Kronberg, E., Grigorenko, E., Clark, G., Vogt, M., & Roussos, E. (2022). Plasmoids in the Jovian magnetotail statistical survey of ion acceleration using Juno. *Journal of Geophysical Research: Space Physics*, *127*(8), 1–17. https://doi.org/10.1029/2022JA030460

Bonfond, B., Yao, Z. H., Gladstone, G. R., Grodent, D., Gérard, J.-C., Matar, J., et al. (2021). Are dawn storms Jupiter's auroral substorms? *AGU Advances*, *2*(1), 1–14. https://doi.org/10.1029/2020AV000275

Clark, G., Tao, C., Mauk, B. H., Nichols, J., Saur, J., Bunce, E. J., et al. (2018). Precipitating electron energy flux and characteristic energies in Jupiter's main auroral region as measured by Juno/JEDI. *Journal of Geophysical Research: Space Physics*, *123*(9), 7554–7567. https://doi.org/10.1029/2018JA025639

Delamere, P. A., Otto, A., Ma, X., Bagenal, F., & Wilson, R. J. (2015). Magnetic flux circulation in the rotationally driven giant magnetospheres. *Journal of Geophysical Research: Space Physics*, *120*(6), 4229–4245. https://doi.org/10.1002/2015JA021036

Frank, L. A., Ackerson, K. L., Lee, J. A., English, M. R., & Pickett, G. L. (1992). The plasma instrumentation for the Galileo mission. *Space Science Reviews*, *60*(1–4), 283–304. https://doi.org/10.1007/BF00216858

Grodent, D. (2015). A brief review of ultraviolet auroral emissions on giant planets. *Space Science Reviews*, *187*(1–4), 23–50. https://doi.org/10.1007/s11214-014-0052-8

Guo, R., & Yao, Z. (2024). Magnetic reconnection in the magnetodisk of centrifugally dominated giant planets. In *Reviews of modern plasma physics*, (Vol. 8, pp. 1–33). Springer Nature. https://doi.org/10.1007/s41614-024-00162-7

Guo, R. L., Yao, Z. H., Dunn, W. R., Palmaerts, B., Sergis, N., Grodent, D., et al. (2021). A rotating azimuthally distributed auroral current system on Saturn revealed by the Cassini spacecraft. *The Astrophysical Journal Letters*, *919*(2), 1–11. https://doi.org/10.3847/2041-8213/ac26b5

Guo, R. L., Yao, Z. H., Grodent, D., Bonfond, B., Clark, G., Dunn, W. R., et al. (2021). Jupiter's double-arc aurora as a signature of magnetic reconnection: Simultaneous observations from HST and Juno. *Geophysical Research Letters*, *48*(14), 1–11. https://doi.org/10.1029/2021GL093964

Guo, R. L., Yao, Z. H., Sergis, N., Wei, Y., Mitchell, D., Roussos, E., et al. (2018b). Reconnection acceleration in Saturn's dayside magnetodisk: A multicase study with Cassini. *The Astrophysical Journal*, *868*(2), 1–8. https://doi.org/10.3847/2041-8213/aaedab

Guo, R. L., Yao, Z. H., Sergis, N., Wei, Y., Xu, X. J., Coates, A. J., et al. (2019). Long-standing small-scale reconnection processes at Saturn revealed by Cassini. *The Astrophysical Journal Letters*, *884*(1), 1–6. https://doi.org/10.3847/2041-8213/ab4429

Guo, R. L., Yao, Z. H., Wei, Y., Ray, L. C., Rae, I. J., Arridge, C. S., et al. (2018a). Rotationally driven magnetic reconnection in Saturn's dayside. *Nature Astronomy*, *2*(8), 640–645. https://doi.org/10.1038/s41550-018-0461-9

Hones, E. W., Jr. (1976). The magnetotail: Its generation and dissipation. In D. J. Williams (Ed.), *Physics of solar planetary environments* (pp. 559–571). AGU.

Hones, E. W., Jr. (1977). Substorm processes in the magnetotail: Comments on "On hot tenuous plasma, fireballs, and boundary layers in the Earth's magnetotail" by L. A. Frank, K. L. Ackerson, & R. P. Lepping. *Journal of Geophysical Research*, *82*(35), 5633–5640. https://doi.org/10.1029/JA082i035p05633

Jackman, C. M., Arridge, C. S., McAndrews, H. J., Henderson, M. G., & Wilson, R. J. (2009). Northward field excursions in Saturn's magnetotail and their relationship to magnetospheric periodicities. *Geophysical Research Letters*, *36*(L16101), 1–5. https://doi.org/10.1029/2009GL039149

Khurana, K. (1997). Euler potential models of Jupiter's magnetospheric field. *Journal of Geophysical Research*, *102*(A6), 11295–11306. https://doi.org/10.1029/97JA00563

Khurana, K. K., Kivelson, M. G., Vasyliunas, V. M., Krupp, N., Woch, J., Lagg, A., et al. (2004). The configuration of Jupiter's magnetosphere. In F. Bagenal, T. E. Dowling, & W. B. Mckinnon (Eds.), *Jupiter: The planet, satellites and magnetosphere* (pp. 593–616). Cambridge University Press.

Kivelson, M. G. (2015). Planetary magnetodiscs: Some unanswered questions. *Space Science Reviews*, *187*(1–4), 5–21. https://doi.org/10.1007/s11214-014-0046-6

Kivelson, M. G., Khurana, K. K., Means, J. D., Russell, C. T., & Snare, R. C. (1992). The Galileo magnetic field investigation. *Space Science Reviews*, *60*(1–4), 357–383. https://doi.org/10.1007/BF00216862

Kivelson, M. G., & Southwood, D. J. (2005). Dynamical consequences of two modes of centrifugal instability in Jupiter's outer magnetosphere. *Journal of Geophysical Research*, *110*(A12), 1–13. https://doi.org/10.1029/2005JA011176

Krimigis, S. M., Armstrong, T. P., Axford, W. I., Bostrom, C. O., Fan, C. Y., Gloeckler, G., & Lanzerotti, L. J. (1977). The low energy charged particle (LECP) experiment on the Voyager spacecraft. *Space Science Reviews*, *21*(3), 329–354. https://doi.org/10.1007/BF00211545

Kronberg, E. A., & Daly, P. W. (2013). Spectral analysis for wide energy channels. *Geoscientific Instrumentation, Methods and Data Systems*, *2*(2), 257–261. https://doi.org/10.5194/gi-2-257-2013

Krupp, N., Vasyliunas, V. M., Woch, J., Lagg, A., Khurana, K. K., Kivelson, M. G., et al. (2004). The dynamics of the Jovian magnetosphere. In F. Bagenal, T. E. Dowling, & W. B. Mckinnon (Eds.), *Jupiter: The planet, satellites and magnetosphere* (pp. 617–638). Cambridge University Press.

Liu, Z.-Y., Zong, Q.-G., Blanc, M., Sun, Y.-X., Zhao, J.-T., Hao, Y.-X., & Mauk, B. H. (2021). Statistics on Jupiter's current sheet with Juno data: Geometry, magnetic fields and energetic particles. *Journal of Geophysical Research: Space Physics*, *126*(11), e2021JA029710. https://doi.org/10.1029/2021JA029710

Mauk, B. H., Mitchell, D. G., McEntire, R. W., Paranicas, C. P., Roelof, E. C., Williams, D. J., et al. (2004). Energetic ion characteristics and neutral gas interactions in Jupiter's magnetosphere. *Journal of Geophysical Research*, *109*(A9), 1–24. https://doi.org/10.1029/2003JA010270

Nakagawa, T., Nishida, A., & Saito, T. (1989). Planar magnetic structures in the solar wind. *Journal of Geophysical Research*, *94*(A9), 11761–11775. https://doi.org/10.1029/JA094iA09p11761

Ness, N. F., Acuña, M. H., Behannon, K. W., Burlaga, L. F., Connerney, J. E. P., Lepping, R. P., & Neubauer, F. M. (1979). Magnetic field studies at Jupiter by Voyager 2: Preliminary results. *Science*, *206*(4421), 966–972. https://doi.org/10.1126/science.206.4421.966

Palmaerts, B., Vogt, M. F., Krupp, N., Grodent, D., & Bonfond, B. (2017). Dawn-dusk asymmetries in Jupiter's magnetosphere. In S. Haaland, A. Runov, & C. Forsyth (Eds.), *Dawn-dusk asymmetries in planetary plasma Environment, Geophysical monograph 230, American geophysical union* (1st ed., pp. 309–322). John Wiley & Sons, Inc.

Thomas, N., Bagenal, F., Hill, T. W., & Wilson, J. K. (2004). The Io neutral clouds and plasma Torus. In F. Bagenal, T. E. Dowling, & W. B. Mckinnon (Eds.), *Jupiter: The tlanet, satellites and magnetosphere* (pp. 561–591). Cambridge University Press.

Vasyliunas, V. M. (1983). Plasma distribution and flow. In A. J. Dessler (Ed.), *Physics of the Jovian magnetosphere* (pp. 395–453). Cambridge University Press. https://doi.org/10.1017/cbo9780511564574.013

Vogt, M. F., Connerney, J. E. P., DiBraccio, G. A., Wilson, R. J., Thomsen, M. F., Ebert, R. W., et al. (2020). Magnetotail reconnection at Jupiter: A survey of Juno magnetic field observations. *Journal of Geophysical Research: Space Physics*, *125*(3), 1–15. https://doi.org/10.1029/2019JA027486

Vogt, M. F., Gyalay, S., Kronberg, E. A., Bunce, E. J., Kurth, W. S., Zieger, B., & Tao, C. (2019). Solar wind interaction with Jupiter's magnetosphere: A statistical study of Galileo in situ data and modeled upstream solar wind conditions. *Journal of Geophysical Research: Space Physics*, *124*(12), 10170–10199. https://doi.org/10.1029/2019JA026950

Vogt, M. F., Jackman, C. M., Slavin, J. A., Bunce, E. J., Cowley, S. W. H., Kivelson, M. G., & Khurana, K. K. (2014). Structure and statistical properties of plasmoids in Jupiter's magnetotail. *Journal of Geophysical Research: Space Physics*, *119*(2), 821–843. https://doi.org/10.1002/2013JA019393

Vogt, M. F., Kivelson, M. G., Khurana, K. K., Joy, S. P., & Walker, R. J. (2010). Reconnection and flows in the Jovian magnetotail as inferred from magnetometer observations. *Journal of Geophysical Research*, *115*(6), 1–19. https://doi.org/10.1029/2009JA015098

Williams, D. J., McEntire, R. W., Jaskulek, S., & Wilken, B. (1992). The Galileo energetic particles detector. *Space Science Reviews*, *60*(1–4), 385–412. https://doi.org/10.1007/BF00216863

Yao, Z. H., Bonfond, B., Clark, G., Grodent, D., Dunn, W. R., Vogt, M. F., et al. (2020). Reconnection-and dipolarization-driven auroral dawn storms and injections. *Journal of Geophysical Research: Space Physics*, *125*(8), e2019JA027663. https://doi.org/10.1029/2019JA027663

Yao, Z. H., Coates, A. J., Ray, L. C., Rae, I. J., Grodent, D., Jones, G. H., et al. (2017a). Corotating magnetic reconnection site in Saturn's magnetosphere. *The Astrophysical Journal*, *846*(2), 1–7. https://doi.org/10.3847/2041-8213/aa88af

Yao, Z. H., Grodent, D., Ray, L. C., Rae, I. J., Coates, A. J., Pu, Z. Y., et al. (2017b). Two fundamentally different drivers of dipolarizations at Saturn. *Journal of Geophysical Research: Space Physics*, *122*(4), 4348–4356. https://doi.org/10.1002/2017JA024060

Zhang, B., Delamere, P. A., Yao, Z., Bonfond, B., Lin, D., Sorathia, K. A., et al. (2021). How Jupiter's unusual magnetospheric topology structures its aurora. *Science Advances*, *7*(15), 1–7. https://doi.org/10.1126/sciadv.abd1204

Zong, Q. G., Fritz, T. A., Pu, Z. Y., Fu, S. Y., Baker, D. N., Zhang, H., et al. (2004). Cluster observations of earthward flowing plasmoid in the tail. *Geophysical Research Letters*, *31*(18), 1–4. https://doi.org/10.1029/2004GL020692